7-2013

Asymmetries in production of $He^+(n = 2)$ with an intense few-cycle attosecond pulse

Jean Marcel Ngoko Djiokap
University of Nebraska-Lincoln, marcelngoko@unl.edu

S. X. Hu
University of Rochester

Wei-Chao Jiang
Peking University

Liang-You Peng
Peking University

Anthony F. Starace
University of Nebraska-Lincoln, astarace1@unl.edu

PHYSICAL REVIEW A **88**, 011401(R) (2013)

Asymmetries in production of $He^+(n = 2)$ with an intense few-cycle attosecond pulse

J. M. Ngoko Djiokap,[1] S. X. Hu,[2] Wei-Chao Jiang,[3] Liang-You Peng,[3] and Anthony F. Starace[1]

[1]*Department of Physics and Astronomy, University of Nebraska, Lincoln, Nebraska 68588-0299, USA*

[2]*Laboratory for Laser Energetics, University of Rochester, Rochester, New York 14623, USA*

[3]*State Key Laboratory for Mesoscopic Physics and Department of Physics, Peking University, Beijing 100871, China*

(Received 26 October 2012; published 8 July 2013)

By solving the two-electron time-dependent Schrödinger equation, we study carrier-envelope-phase (CEP) effects on ionization plus excitation of He to $He^+(n = 2)$ states by a few-cycle attosecond pulse with a carrier frequency of 51 eV. For most CEPs the asymmetries in the photoelectron angular distributions with excitation of $He^+(2s)$ or $He^+(2p)$ have opposite signs and are two orders of magnitude larger than for ionization without excitation. These results indicate that attosecond pulse CEP effects may be significantly amplified in correlated two-electron ionization processes.

DOI: 10.1103/PhysRevA.88.011401 PACS number(s): 32.80.Fb, 02.70.Dh, 32.80.Rm, 32.80.Zb

A main goal of attosecond science is to control electronic motion on its natural time scale [1–4]. A milestone toward achieving such control is the experimental realization of few-cycle attosecond pulses with stable carrier envelope phases (CEPs) [5–7]. A possible method for tuning the CEP has also been proposed [5]. For few-cycle IR pulses, it has long been predicted [8] and confirmed experimentally [9–12] that the angular distribution of ionized electrons can be asymmetric in certain energy ranges and for certain CEPs. Such asymmetries may be understood as mimicking the asymmetry of the electric field of a few-cycle laser pulse [9–12]. More fundamentally, the asymmetries may be regarded as stemming from the large bandwidth of a few-cycle laser pulse, which results in overlapping transition amplitudes to states of different parity; i.e., owing to the large bandwidth, transition amplitudes for ionization involving N or $N + 1$ photons of the carrier frequency may overlap in energy [8,13–16].

For a few-cycle XUV attosecond pulse, the bandwidth of the pulse can be the same order of magnitude as the XUV carrier frequency, thus indicating the possibility of controlling electronic motion over a large range of electron energy [15–17]. Realization of this possibility, however, requires much more intense attosecond pulses than currently exist so that nonlinear attosecond processes are significant. Theory indicates that attosecond pulse peak intensities of order 1 PW/cm^2 are necessary [15–17]. While such intensities are not yet a reality, experimental progress toward increasing the intensity of XUV attosecond pulses is being made (see, e.g., Refs. [18–22]).

Most experimental work (e.g., Refs. [9–12]) concerning CEP effects on ionized electron angular distributions has been for single-electron ionization processes and, consequently, nearly all theoretical works on few-cycle pulse ionization processes have made use of the single active electron (SAE) approximation. We recently investigated the CEP effects of a few-cycle XUV attosecond pulse on single ionization of He to the $He^+(1s)$ state by solving the two-electron time-dependent Schrödinger equation (TDSE) [23] in order to compare our results with prior results using the SAE approximation [15]. We found that doubly excited states of He influence significantly the CEP-induced asymmetry of the ionized electron angular distribution, despite the large bandwidth of the XUV attosecond pulse. Given this evidence [23] of two-electron effects on a basically single-electron ionization process, we were motivated in this work to investigate the CEP effects of a few-cycle attosecond pulse on a strictly two-electron ionization process (i.e., ionization plus excitation) for the fundamental two-electron atom, He. Ionization plus excitation is a two-electron process (i.e., one that cannot be described using the SAE approximation) that allows an essentially exact quantum-mechanical numerical analysis for He. Moreover, for few-cycle XUV pulses (as opposed to few-cycle IR pulses), numerical results can be compared with a perturbative theoretical analysis of attosecond photoionization involving only first- and second-order transition amplitudes [16].

In this Rapid Communication, we present theoretical results on photoelectron angular distribution asymmetries in single ionization plus excitation (SIE) of He to $He^+(2s,2p)$ states by a few-cycle, linearly polarized, attosecond pulse defined by its vector potential $\mathbf{A}(t)$ and electric field $\mathbf{E}(t)$:

$$\mathbf{A}(t) = A_0 f(t) \sin(\omega t + \varphi)\mathbf{e}_z, \quad \mathbf{E}(t) = -\frac{\partial}{\partial t}\mathbf{A}(t), \qquad (1)$$

where φ is the CEP and $f(t)$ is the pulse envelope. We assume that $f(t)$ has a cosine-squared shape, $\cos^2(\pi t/T)$, over the interval $-T/2 \leqslant t \leqslant T/2$, where T is the total pulse duration, equal to an integer number n_c of optical cycles [$T \equiv n_c(2\pi/\omega)$]. The peak intensity of the pulse is $I = E_0^2$, where $E_0 \equiv A_0\omega$, the temporal FWHM of its intensity profile is $0.364T$, and its spectral width is $1.44\omega/n_c$ [24]. In our calculations we have chosen $I = 1$ or 2 PW/cm^2, $\omega = 51$ eV, and pulse lengths $T = 162$ as (2-cycles) or 243 as (3-cycles). The FWHM in the intensity for $T = 3$ -cycles is 1.1 cycles, which is comparable to those of the single-cycle pulses achieved experimentally [5,6]. For SIE of He to $He^+(n = 2)$, the threshold energy is 65.41 eV. Although the carrier frequency ω of our pulse is below this threshold, the bandwidth of 36.7 eV for $T = 2$-cycles (or 24.5 eV for $T = 3$-cycles) ensures that there is significant overlap of first- and second-order SIE amplitudes (of comparable magnitudes) in the energy region above the $He^+(n = 2)$ threshold.

For few-cycle attosecond pulses, the SIE cross section is not meaningful owing to the broad pulse bandwidth. The relevant observable is the probability for SIE of He to

$He^+(2s,2p)$, which is obtained by projecting the two-electron wave packet (after the interaction with the pulse) onto field-free, correlated wave functions. Our numerical methods for obtaining the two-electron wave packet and the field-free correlated wave functions are presented in detail in Ref. [23], which considered ionization without excitation of He. In brief, two methods were used to solve the full-dimensional, two-electron TDSE to obtain the continuum part of the two-electron wave packet $\Phi_C(\varphi)$: (1) a TDSE parallel solver combining the real-space-product algorithm with a finite-element discrete-variable representation (FE-DVR) [25,26]; (2) a two-electron TDSE method [27] using normalized Gauss-Lobatto FE-DVR basis functions [28,29] and an iterative Arnoldi-Lanczos method [30]. Both methods give the same converged results. The field-free SIE states of He are described by a multichannel scattering wave function $\Theta_\Gamma(E,\hat{\mathbf{k}}_e)$ obtained accurately using the Jacobi- or J-matrix method [23,31–38]. In each final state channel Γ, the wave function is expanded in a basis of Coulomb-Sturmian functions [23]. The channel $\Gamma \equiv (n,l,l';LM)$ designates respectively the $He^+(nl)$ radial and angular momentum quantum numbers (where $nl = 2s$ or $2p$), the angular momentum l' of the ionized electron, and the total angular momentum L and its projection M, where $M = 0$ for a linearly polarized pulse. Owing to azimuthal symmetry, the dependence on the ionized electron's momentum direction $\hat{\mathbf{k}}_e$ reduces to dependence on the angle θ with respect to the laser polarization axis (our z axis). In this work, we present results only for electron ionization in the forward ($\theta_+ = 0$) and backward ($\theta_- = \pi$) directions, for which the asymmetry is largest.

The differential probability density for SIE of He to $He^+(nl)$ with the photoelectron having energy E is

$$P_{nl}(E,\theta_\pm,\varphi) = |\langle\Phi_C(\varphi)|\sum_{l'L}\Theta_\Gamma(E,\theta_\pm)\rangle|^2. \quad (2)$$

For a given CEP φ, the asymmetry $\Delta P_{nl}(E,\varphi)$ for electron ionization along $\theta_\pm$ is [15,23]

$$\Delta P_{nl}(E,\varphi) = P_{nl}(E,\theta_+,\varphi) - P_{nl}(E,\theta_-,\varphi). \quad (3)$$

The normalized asymmetry factor is defined as

$$R_{nl}(E,\varphi) = \Delta P_{nl}(E,\varphi)/[P_{nl}(E,\theta_+,\varphi) + P_{nl}(E,\theta_-,\varphi)]. \quad (4)$$

In our calculations, four values of the total angular momentum are included: $0 \leqslant L \leqslant 3$. Even for a peak pulse intensity of 2 PW/cm^2 it is useful to analyze the nonperturbative TDSE results in terms of the key contributing perturbation theory terms (in the electron-laser pulse interaction) [16]. By electric dipole selection rules, the first-order transition amplitude produces final states with $^1P^o$ symmetry, while the second-order transition amplitude produces final states with either $^1S^e$ or $^1D^e$ symmetry. Owing to the different parities of the first- and second-order transition amplitudes, they interfere constructively on one side of the z axis and destructively on the other. The third-order transition amplitude produces either $^1P^o$ or $^1F^o$ final states; these are included, but their contributions are small. For photoelectron energies $0.1 \leqslant E \leqslant 30$ eV, we find that for either ion state ($2s$ or $2p$) the odd-parity $^1P^o$ (first order ≈1-photon) amplitude (which is nonzero above the SIE threshold owing to the bandwidth of the pulse) is not much larger in magnitude than the even parity $^1S^e$ or $^1D^e$ (second order ≈ 2-photon) amplitudes. The interference between these ≈1- and ≈2-photon amplitudes is seen in the inset graphs of Fig. 1 in which many autoionizing resonances with different parities are visible in the SIE probability density spectrum [see Eq. (2)]. Results in Fig. 1 for the differential probability density are obtained by projecting the wave-packet solutions of the two-electron TDSE onto the correlated J-matrix (CJM) field-free states.

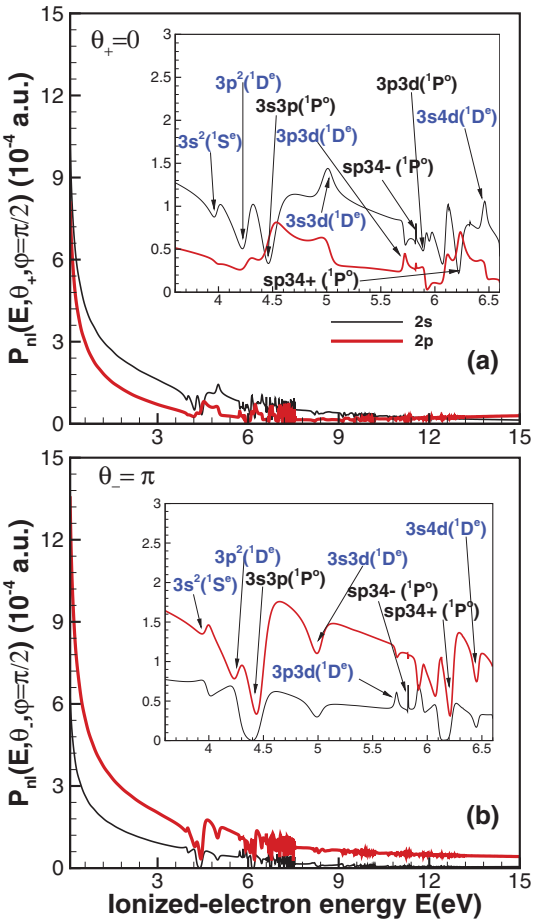

FIG. 1. (Color online) Differential probability density [Eq. (2)] for SIE of He to $He^+(2s,2p)$ by a 3-cycle pulse (with $\omega = 51$ eV, CEP $\varphi = \pi/2$, and peak pulse intensity $I = 2$ PW/cm^2) for (a) forward ($\theta_+ = 0$) and (b) backward ($\theta_- = \pi$) electron ejection with kinetic energy $0.1 \leqslant E \leqslant 15.0$ eV. The inset figures show the doubly excited state features in the energy region $3.6 \leqslant E \leqslant 6.6$ eV.

In Fig. 2 we compare the asymmetry $\Delta P_{nl}(E,\varphi)$ [see Eq. (3)] for SIE produced by 2- and 3-cycle pulses having a CEP $\varphi = \pi/2$ for photoelectron energies $0.1 \leqslant E \leqslant 15.0$ eV. The asymmetries for the $He^+(2s,2p)$ states have opposite signs, and are approximately mirror images of one another. The sign of the asymmetry for $He^+(2s)$ is the same as that found [23] for ionization of He without excitation, i.e., for the $He^+(1s)$ state. Our correlated calculations include many interacting channels: for first- and second-order SIE processes, there are three open channels for each of the $He^+(1s)$ and $He^+(2s)$ states, and five open channels for the $He^+(2p)$ state. From a perturbation theory analysis [16], the asymmetry $\Delta P_{nl}(E,\varphi)$ is proportional to the interference of the first- and second-order amplitudes, i.e., $\mathrm{Re}(A^{(1)}_{nl} A^{(2)*}_{nl})$. Whereas $A^{(1)}_{2s}$ and

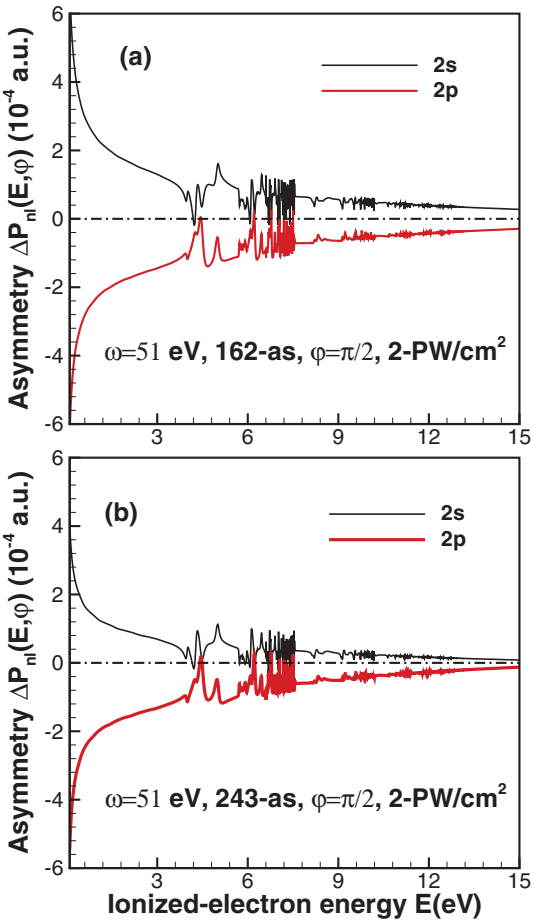

FIG. 2. (Color online) Asymmetry $\Delta P(E,\varphi)$ [Eq. (3)] vs E for SIE of He to $He^+(2s,2p)$ by (a) 2-cycle and (b) 3-cycle attosecond pulses, with other pulse parameters as in Fig. 1.

$A_{2p}^{(1)}$ have opposite signs over a large range of electron energy, $A_{2s}^{(2)}$ and $A_{2p}^{(2)}$ have the same signs. Also, while the phases of the first- and second-order amplitudes for $2s$ are comparable, those for $2p$ differ by ≈ 2 rad.

For energies near threshold, $E \leqslant 5$ eV, the asymmetries $\Delta P(E,\varphi)$ [see Eq. (3)] are largest, indicating that for the XUV pulse parameters we have chosen, the overlap of the first- and second-order transition amplitudes, $\mathrm{Re}(A_{nl}^{(1)} A_{nl}^{(2)*})$, is largest in this energy region. The 2- and 3-cycle results are similar, differing primarily in magnitude (with the shorter pulse producing higher absolute asymmetries). Regardless of the number of cycles, while the asymmetries generally decrease with increasing energy E, one finds significant enhancement or suppression of the asymmetry in the vicinity of autoionizing states over an energy scale comparable to their widths.

In Figs. 3(a) and 3(b) we plot the CEP dependence of the energy-integrated asymmetries $\Delta P_{nl}(\varphi) \equiv \int \Delta P_{nl}(E,\varphi) dE$ for the cases of a 2-cycle and a 3-cycle pulse. For both pulses, $\Delta P_{nl}(\varphi)$ has a convex shape for $2p$ and a concave shape for $2s$. For most CEPs, $\Delta P_{n=2}(\varphi) = \Delta P_{2s}(\varphi) + \Delta P_{2p}(\varphi)$ for $He^+(n = 2)$ is smaller in magnitude than those for $He^+(2s)$ and $He^+(2p)$, but can be larger near $\varphi \approx 0$ or π. Regardless of the pulse length, $\Delta P_{nl}(\varphi)$ is larger for $I = 2\ \mathrm{PW/cm^2}$ (see Fig. 3)

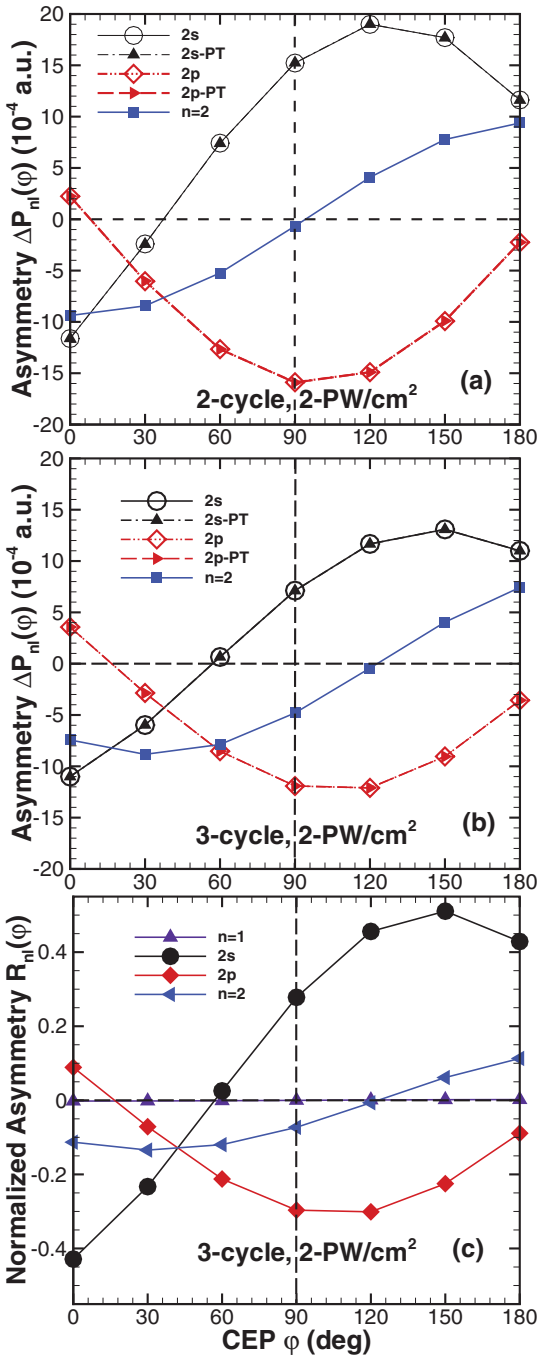

FIG. 3. (Color online) CEP dependence of the energy-integrated asymmetries $\Delta P_{nl}(\varphi)$ for SIE of He to $He^+(2s,2p)$ states by (a) 2-cycle and (b) 3-cycle pulses, with other parameters as in Fig. 1. Our CJM results are compared to the perturbation theory (PT) parametrization of Ref. [16]. (c) Comparison of the energy-integrated normalized asymmetries $R_{2s}(\varphi)$, $R_{2p}(\varphi)$, and $R_{n=2}(\varphi)$ with $R_{n=1}(\varphi)$ for 3-cycle pulses.

than for $I = 1\ \mathrm{PW/cm^2}$ (not shown). In Fig. 3(c) we show for the 3-cycle case the CEP dependence of the energy-integrated normalized asymmetries $R_{nl}(\varphi)$ [defined as the ratio of the energy-integrated numerator and denominator in Eq. (4)] and $R_{n=2}(\varphi) \equiv \Delta P_{n=2}(\varphi)/[P_{n=2}(\theta_+,\varphi) + P_{n=2}(\theta_-,\varphi)]$. Whereas the maximum magnitude of $R_{2p}(\varphi)$ occurs at $\varphi \approx 120^\circ$ and equals -30%, that for the $2s$ state is at $\varphi \approx 150^\circ$ and equals

TABLE I. Parameters $|K_{2s,2p}|$ (10^{-4} a.u.) and $\Theta_{K_{2s,2p}}$ (deg) obtained by fitting Eq. (5) (with $I_0 = 2$ PW/cm^2) to our 2- and 3-cycle CJM data for $I = 1$ and 2 PW/cm^2.

Pulse:	162 as/1-PW	162 as/2-PW	243 as/1-PW	243 as/2-PW
$\|K_{2s}\|$	19.153	19.163	13.126	13.103
$\Theta_{K_{2s}}$	127.07	127.27	146.92	147.12
$\|K_{2p}\|$	16.158	16.067	12.477	12.434
$\Theta_{K_{2p}}$	277.40	278.02	285.43	286.68

+51%, while that for $n = 2$ is at $\varphi \approx 30^\circ$ and equals −13%. The magnitudes of $R_{2s}(\varphi)$ and $R_{2p}(\varphi)$ are two orders of magnitude larger than $R_{n=1}(\varphi)$ for single ionization without excitation [see Fig. 3(c)]. For our SIE process, $\omega = 51$ eV is below the $He^+(n = 2)$ threshold, whereas it is well above the $He^+(1s)$ threshold; hence the interference of first- and second-order amplitudes occurs in different energy regions relative to these thresholds. The correlated SIE process thus amplifies the asymmetry.

For the peak pulse intensities employed in this work, time-dependent perturbation theory in powers of the attosecond pulse electric field may be used to parametrize the asymmetry in the SIE spectrum [16,23]. Including terms up to second order in the pulse field, the CEP dependence of $\Delta P_{nl}(\varphi)$ has the form [16]

$$\Delta P_{nl}(\varphi) = |K_{nl}|(I/I_0)^{3/2}\cos(\varphi - \Theta_{K_{nl}}), \qquad (5)$$

where $K_{nl} \equiv |K_{nl}|\exp(i\Theta_{K_{nl}})$ is a complex dynamical parameter independent of φ and the dependence on intensity I (relative to some reference intensity I_0) is shown explicitly. Table I shows these parameters for $nl = 2s,2p$ obtained by fitting Eq. (5) to our numerical CJM data. For a given pulse duration, both $|K_{2l}|$ and the phase angle $\Theta_{K_{2l}}$ are relatively insensitive to the pulse intensity. As shown in Figs. 3(a) and 3(b), the fit of Eq. (5) to our CJM data for two different pulse durations is excellent.

The implication of Eq. (5) for experiment is that uncertainty in the peak pulse intensity I only affects the magnitude of $\Delta P_{nl}(\varphi)$ and not the shape of its φ dependence. Also, estimates for $\Delta P_{2p}(\varphi)$ [for laser parameters as in Fig. 2(a)] with electrons ejected at a small angle relative to the z axis [i.e., $0^\circ \leqslant \theta_+ \leqslant 10^\circ$, $\theta_- = 180^\circ - \theta_+$, see Eq. (3)] show that $\Delta P_{2p}(\varphi)$ is nearly constant (to within 1.5% at $\theta_+ = 10^\circ$). We thus expect that the CJM results in Fig. 3 are essentially constant for electrons ejected within a few degrees of the z axis. Finally, although distinguishing excitations to the $2s$ or $2p$ states requires detection of fluorescence from these states [39–41], Fig. 3 shows that $\Delta P_{n=2}(\varphi)$ is significant for both pulse durations and that $R_{n=2}(\varphi)$ is far larger than $R_{n=1}(\varphi)$. Moreover, Woodruff and Samson [42] have shown that the fluorescence signal from $He^+(n = 2)$ dominates over those from all higher excited states combined, being approximately five times larger. This is consistent with our own CJM results for the integrated asymmetry $\Delta P_{n=3}$ for $\varphi = \pi/2$, which we find is about six times smaller than for $\Delta P_{n=2}$ for the same CEP.

In summary, we have shown by essentially exact numerical calculations for the fundamental two-electron He atom that multielectron processes initiated by an intense few-cycle attosecond pulse permit a much greater possibility for control of electronic motion by means of the CEP of the pulse. Specifically, the asymmetries for ionization with excitation of $He^+(2s,2p)$ are two orders of magnitude larger than that for ionization without excitation [see Fig. 3(c)]. Moreover, these asymmetries differ in sign for $2s$ and $2p$. In addition, we have shown (see Table I) that certain dynamical parameters [16] (which provide information on the ionization plus excitation process) are relatively insensitive to pulse intensity, thus making their measurement experimentally feasible. These features stem from the nonlinearity of the attosecond process we have investigated. Progress in increasing attosecond pulse intensities will make such studies of nonlinear attosecond processes an experimental reality.

We thank Bernard Piraux for helpful discussions. This work is supported in part by DOE, Office of Science, Division of Chemical Sciences, Geosciences, and Biosciences, Grant No. DE-FG03-96ER14646; by the Laboratory for Laser Energetics, University of Rochester; and by the National Natural Science Foundation of China, Grants No. 11174016 and No. 11121091. Results were obtained using the Merritt facility at the Holland Computing Center, University of Nebraska; the NSF TeraGrid resources on the NICS Kraken supercomputer, Grants No. TG-PHY-100052, No. TG-PHY-120003, No. TG-PHY-110003, and No. TG-PHY-110009; and the computer cluster "MESO," State Key Laboratory for Mesoscopic Physics, Peking University.

[1] P. B. Corkum and F. Krausz, Nat. Phys. **3**, 381 (2007).
[2] F. Krausz and M. Ivanov, Rev. Mod. Phys. **81**, 163 (2009).
[3] M. Nisoli and G. Sansone, Prog. Quantum Electron. **33**, 17 (2009).
[4] G. Sansone, L. Poletto, and M. Nisoli, Nat. Photon. **5**, 655 (2011).
[5] G. Sansone *et al.*, Science **314**, 443 (2006).
[6] E. Goulielmakis *et al.*, Science **320**, 1614 (2008).
[7] F. Calegari, M. Lucchini, M. Negro, C. Vozzi, L. Poletto, O. Svelto, S. DeSilvestri, G. Sansone, S. Stagira, and M. Nisoli, J. Phys. B **45**, 074002 (2012).
[8] E. Cormier and P. Lambropoulos, Eur. Phys. J. D **2**, 15 (1998).
[9] G. G. Paulus, F. Grasbon, H. Walther, P. Villorese, M. Nisoli, S. Stagira, E. Priori, and S. De Silvestri, Nature **414**, 182 (2001)
[10] G. G. Paulus, F. Lindner, H. Walther, A. Baltuška, E. Goulielmakis, M. Lezius, and F. Krausz, Phys. Rev. Lett. **91**, 253004 (2003).
[11] D. B. Milošević, G. G. Paulus, D. Bauer, and W. Becker, J. Phys. B **39**, R203 (2006).
[12] M. F. Kling, J. Rauschenberger, A. J. Verhoef, E. Hasović, T. Uphues, D. B. Milošević, H. G. Muller, and M. J. J. Vrakking, New J. Phys. **10**, 025024 (2008).
[13] A. Gürtler, F. Robicheaux, W. J. van der Zande, and L. D. Noordam, Phys. Rev. Lett. **92**, 033002 (2004).

[14] V. Roudnev and B. D. Esry, Phys. Rev. Lett. **99**, 220406 (2007).
[15] L.-Y. Peng, E. A. Pronin, and A. F. Starace, New J. Phys. **10**, 025030 (2008).
[16] E. A. Pronin, A. F. Starace, M. V. Frolov and N. L. Manakov, Phys. Rev. A **80**, 063403 (2009).
[17] E. A. Pronin, A. F. Starace, and L.-Y. Peng, Phys. Rev. A **84**, 013417 (2011).
[18] S. Gilbertson, Y. Wu, S. D. Khan, M. Chini, K. Zhao, X. Feng, and Z. Chang, Phys. Rev. A **81**, 043810 (2010).
[19] E. J. Takahashi, P. Lan, O. D. Mücke, Y. Nabekawa, and K. Midorikawa, Phys. Rev. Lett. **104**, 233901 (2010).
[20] F. Ferrari, F. Calegari, M. Lucchini, C. Vozzi, S. Stagira, G. Sansone, and M. Nisoli, Nat. Photon. **4**, 875 (2010).
[21] T. Popmintchev, M.-C. Chen, P. Arpin, M. M. Murnane, and H. C. Kapteyn, Nat. Photon. **4**, 822 (2010).
[22] P. Tzallas, E. Skantzakis, L. A. A. Nikolopoulos, G. D. Tsakiris, and D. Charalambidis, Nat. Phys. **7**, 781 (2011).
[23] J. M. Ngoko Djiokap, S. X. Hu, W.-C. Jiang, L.-Y. Peng, and A. F. Starace, New J. Phys. **14**, 095010 (2012).
[24] E. Foumouo, A. Hamido, Ph. Antoine, B. Piraux, H. Bachau, and R. Shakeshaft, J. Phys. B **43**, 091001 (2010).
[25] B. I. Schneider, L. A. Collins, and S. X. Hu, Phys. Rev. E **73**, 036708 (2006).
[26] S. X. Hu, Phys. Rev. E **81**, 056705 (2010).
[27] Z. Zhang, L.-Y. Peng, M.-H. Xu, A. F. Starace, T. Morishita, and Q. Gong, Phys. Rev. A **84**, 043409 (2011).
[28] T. N. Rescigno and C. W. McCurdy, Phys. Rev. A **62**, 032706 (2000).
[29] M. J. Rayson, Phys. Rev. E **76**, 026704 (2007).
[30] Y. Saad, *Numerical Methods For Large Eigenvalue Problems* (Halsted, New York, 1992).
[31] E. J. Heller and H. A. Yamani, Phys. Rev. A **9**, 1201 (1974).
[32] H. A. Yamani and L. Fishman, J. Math. Phys. **16**, 410 (1975).
[33] J. T. Broad and W. P. Reinhardt, Phys. Rev. A **14**, 2159 (1976).
[34] R. Gersbacher and J. T. Broad, J. Phys. B **43**, 365 (1990).
[35] E. Foumouo, G. L. Kamta, G. Edah, and B. Piraux, Phys. Rev. A **74**, 063409 (2006).
[36] *The J-matrix Method: Developments and Applications*, edited by A. D. Alhaidari, E. J. Heller, H. A. Yamani, and M. S. Abdelmonem (Springer, New York, 2008).
[37] J. M. Ngoko Djiokap, E. Foumouo, M. G. Kwato Njock, X. Urbain, and B. Piraux, Phys. Rev. A **81**, 042712 (2010).
[38] Yu.V. Popov, S. A. Zaytsev, and S. I. Vinitsky, Phys. Part. Nucl. **42**, 683 (2011).
[39] P. R. Woodruff and J. A. R. Samson, Phys. Rev. A **25**, 848 (1982).
[40] J. R. Harries, J. P. Sullivan, S. Obara, P. Hammond, and Y. Azuma, J. Phys. B **36**, L319 (2003).
[41] J. R. Harries, J. P. Sullivan, S. Obara, Y. Azuma, J. G. Lambourne, F. Penent, R. I. Hall, P. Lablanquie, K. Bucar, M. Zitnik, and P. Hammond, J. Phys. B **38**, L153 (2005).
[42] P. R. Woodruff and J. A. R. Samson, Phys. Rev. Lett. **45**, 110 (1980).